

Microfluidic immunoassay for detection of serological antibodies: A potential tool for rapid evaluation of immunity against SARS-CoV-2



Cite as: Biomicrofluidics 14, 061507 (2020); doi: 10.1063/5.0031521

Submitted: 1 October 2020 · Accepted: 23 November 2020 ·

Published Online: 14 December 2020



View Online



Export Citation



CrossMark

Hogi Hartanto,¹ Minghui Wu,¹ Miu Ling Lam,² and Ting-Hsuan Chen^{1,a)}

AFFILIATIONS

¹Department of Biomedical Engineering, City University of Hong Kong, Hong Kong Special Administrative Region 999077, China

²School of Creative Media, City University of Hong Kong, Hong Kong Special Administrative Region 999077, China

Note: This paper is part of the special issue on Microfluidic Detection of Viruses for Human Health

a) Author to whom correspondence should be addressed: thchen@cityu.edu.hk

ABSTRACT

In December 2019, coronavirus disease 2019 became a pandemic affecting more than 200 countries and territories. Millions of lives are still affected because of mandatory quarantines, which hamstring economies and induce panic. Immunology plays a major role in the modern field of medicine, especially against virulent infectious diseases. In this field, neutralizing antibodies are heavily studied because they reflect the level of infection and individuals' immune status, which are essential when considering resumption of work, flight travel, and border entry control. More importantly, it also allows evaluating the antiviral vaccine efficacy as vaccines are still known for being the ultimate intervention method to inhibit the rapid spread of virulent infectious diseases. In this Review, we first introduce the host immune response after the infection of SARS-CoV-2 and discuss the latest results using conventional immunoassays. Next, as an enabling platform for detection with sufficient sensitivity while saving analysis time and sample size, the progress of microfluidic-based immunoassays is discussed and compared based on surface modification, microfluidic kinetics, signal output, signal amplification, sample matrix, and the detection of anti-SARS-CoV-2 antibodies. Based on the overall comparison, this Review concludes by proposing the future integration of visual quantitative signals on microfluidic devices as a more suitable approach for general use and large-scale surveillance.

Published under license by AIP Publishing. <https://doi.org/10.1063/5.0031521>

I. INTRODUCTION

At the end of 2019, a novel coronavirus disease 2019 (COVID-19) outbreak had spread rapidly around the world, resulting in a severe global ongoing pandemic. The novel coronavirus, SARS-CoV-2, attacks the lower respiratory system to cause viral pneumonia, which is similar to the Severe Acute Respiratory Syndrome (SARS) in 2002–2003 and Middle East Respiratory Syndrome (MERS) in 2011.^{1,2} The infection of SARS-CoV-2 may also affect the gastrointestinal system, heart, kidney, liver, and central nervous system, leading to multiple organ failures.^{2,3} Importantly, while not as lethal as the SARS and MERS, the SARS-CoV-2 is far more transmissible.⁴ The SARS in 2003 has 8098 reported cases and 774 deaths, and MERS in 2012 has caused 2494 reported cases and 858 deaths. In contrast, the number of infections of SARS-CoV-2 has reached 14 million with 600 000

deaths in the world in six months and continues to grow rapidly.^{3,5,6}

What makes SARS-CoV-2 much more transmissible than other epidemic viruses such as SARS-CoV and MERS-CoV? First, SARS-CoV-2 has a long incubation time. The median incubation is estimated to be 5.1 days, while 97.5% of infected people display symptoms after 11.5 days.⁷ At the same time, the viral load grows since the infection until it peaks a week after the symptom onset,⁸ therefore allowing a longer time for virus spreading and transmission. Second, SARS-CoV-2 infection is much less lethal. The mortality rate of SARS-CoV-2 infection is strongly dependent on the age, where fatality and morbidity are exclusively seen in the age over 50.⁴ For younger generations, a significant proportion of infection is either asymptomatic or with mild illness. As such, long incubation and mild or even no symptom in young infected people

allows more frequent and efficient contagiousness and transmission.

To slow down the spread of the virus, there are increasing demands of the effective diagnosis of COVID-19, and polymerase chain reaction (PCR) has been regarded as a gold standard.⁹ However, due to the cost and limited medical resources, PCR-based mass screening is impractical. Instead, policies were made to close borders and constrain public movements as a result of mandatory isolations/quarantines for preventing further spread of the disease in the community,^{10,11} which hamstring economies, causing fears and panic. As such, alternative solutions are being sought to cope with this situation.

II. HUMAN IMMUNE RESPONSES

The host response is essential for epidemiological control, vaccination, and formulating antiviral strategies against COVID-19. The beta-coronavirus genome of SARS-CoV-2 encodes several structural proteins, including the nucleocapsid protein, transmembrane glycoprotein, envelop protein, and the glycosylated spike protein.^{12,13} When the virus invades, the glycoproteins of the virus structure such as spike protein and nucleocapsid protein would trigger the immune system for producing IgG/IgM antibodies against them. As such, most studies are focusing on the temporal profile of serum antibody responses against spike protein and nucleocapsid protein during the infection of the SARS-CoV-2.⁸

However, different antibodies arising from different antigens imply varied neutralizing activity. Evidence have suggested that antibodies against virus envelope glycoproteins possess important functions including virus neutralization. For example, the spike protein, serving as a pivotal role in infection and pathogenesis, mediates host cell invasion via binding to a receptor protein called angiotensin-converting enzyme 2 (ACE2) located on the surface membrane of the host cells.^{14–16} Thus, the binding of virus antibodies to the virus envelope glycoproteins would impair the binding affinity of the virus to the cell receptor, e.g., SARS-CoV-2 spike protein to ACE2.¹⁷ As a comparison, because nucleocapsid protein is internal to the viral envelope, the role of its antibodies on the neutralization of the live virus has not been established.¹⁷

The neutralizing activity of antibodies makes them suitable candidates for reflecting the level of infection as well as the immune status. Studies of serum antibody responses during the infection of SARS-CoV-2 indicate a growing level of IgG and IgM antibodies in 10 days after the symptom onset, and a more vigorous response of IgG was observed in severe cases than that in mild cases.¹⁸ Importantly, most patients developed seroconversion,⁸ and a higher level of IgG antibody was observed in survivors of the intensive care unit.¹⁹ Using SARS-CoV patients as a reference, such a neutralizing activity may exist for 17 years.²⁰ In addition, while there are reports on the reinfection of SARS-CoV-2, it is believed that reinfection cases might not be due to the genetic mutation of the SARS-CoV-2 virus.²⁰ Instead, the RT-PCR test results from patients who have recovered from COVID-19 might be attributed to the virus which was not totally eradicated from the body, cross-contamination from another beta-coronavirus, false positive results, and incorrect sample collection.²¹ Thus, IgG and IgM antibodies

against the SARS-CoV-2 can still be a feasible biomarker for evaluating the immunity to COVID-19.

As such, there are growing interests and demands of the IgG/IgM antibody test so that people can be aware and document the immune status, which is required before resuming the work, flight travel, border entry control, and so on. It also provides the level of population immunity for public policymakers based on the percentage asymptomatic infected cases in a population. Furthermore, it can be also used to evaluate the efficacy of the vaccine during clinical trials.

III. CONVENTIONAL APPROACH FOR THE DETECTION OF ANTIBODIES

Immunoassay plays a major role to quantify antibodies or neutralizing antibodies.^{22,23} As there are different IgG/IgM antibodies classified based on its glycoprotein antigen, the first concern is to ensure that the IgG/IgM antibody test is specific to SARS-CoV-2 and has no cross-reactivity to other coronaviruses. Cryo-EM (Cryogenic Electron Microscopy) structure analysis has revealed that the binding affinity of SARS-CoV-2 spike protein to ACE2 is about 10–20 times higher than that of the SARS-CoV spike protein.^{12,24} More importantly, a recent study tackling the antigenic differences between SARS-CoV-2 and SARS-CoV shows that, although cross-reactive binding was observed, cross-neutralization of the live viruses was not as common.²⁵ Thus, while the nucleocapsid protein is abundant, the uniqueness of the spike protein further ascertains the specificity of the detection on the neutralizing antibody of SARS-CoV-2.

While both IgG and IgM antibodies to spike protein strongly correlate with virus neutralization,⁸ their presence in serum is in different phases after infection, which raises concerns about the appropriate time for collecting blood samples for serological tests. In a recent article in *The Lancet Infectious Diseases*,⁸ To and colleagues reported the temporal profile of serum antibody responses during the infection of SARS-CoV-2. It is shown that, after the onset of symptoms, IgM antibodies were detected since day 4 and peaked at day 20, while IgG antibodies were detected since day 7 and peaked at approximately day 25.¹⁸ Thus, early detection may subject to insufficient sensitivity and false negativity. Recently, a systematic analysis of antibody detection has revealed that the detection of IgG antibodies provides better sensitivity for samples collected a week after the onset of symptoms,²² and such finding corroborates early results of a lower specificity of IgM tests.²⁶ On the other hand, the combined IgG/IgM test would generally increase the sensitivity irrespective of detection methods.²² Taking together, the combined detection of IgG/IgM against the SARS-CoV-2 spike protein seems to be a better choice considering the sensitivity, specificity, reduced cross-activity, and quantification of virus neutralization.

The next question is to choose the detection principle. The most commonly used immunoassays are Enzyme-Linked Immunosorbent Assay (ELISA), Chemiluminescence Enzyme Immunoassays (CLIA), Fluorescence Immunoassays (FIAs), and the Lateral Flow Immunoassays (LFIA)^{22,23,27,28} (Fig. 1). All methods are designed based on immunoaffinity binding, where the target IgG/IgM antibody simultaneously binds to an anti-human

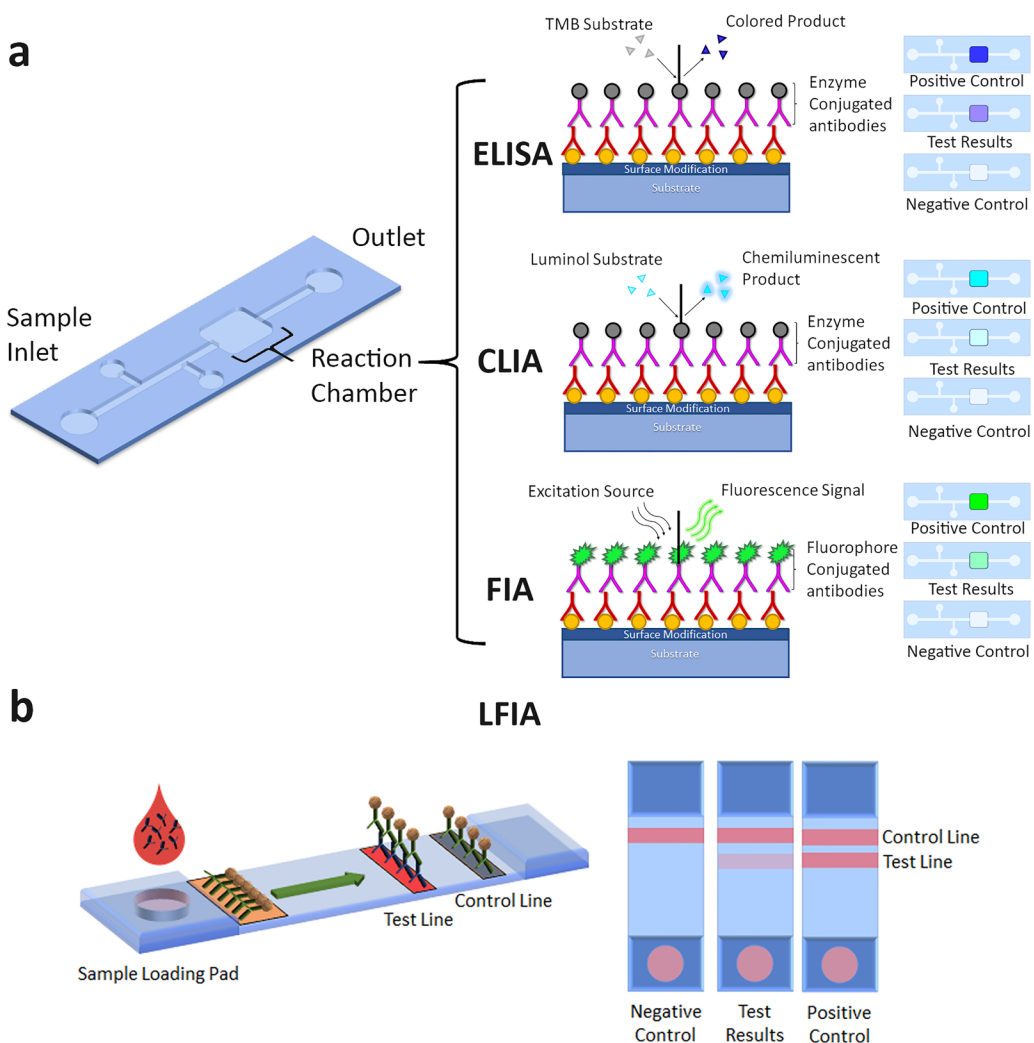


FIG. 1. Immunoassay for antibody detection based on (a) Enzyme-Linked Immunosorbent Assay (ELISA), Chemiluminescence Enzyme Immunoassays (CLIA), Fluorescence Immunoassays (FIAs), and (b) Lateral Flow Immunoassays (LFIA). For ELISA, CLIA, and FIA, similar immunoaffinity binding is used, while the secondary anti-human IgG/IgM antibody is conjugated with an enzyme (ELISA or CLIA) or a fluorescence tag (FIA) that reports optical signals. For LFIA, the presence of target antibody is reported by the appearance of a color band formed by the target-mediated immobilization of nanoparticles.

IgG/IgM antibody and a SARS-CoV-2 antigen, e.g., virus spike protein or nucleocapsid protein. Mostly, the SARS-CoV-2 antigen is to capture the target IgG/IgM antibody against the viral protein, while the other anti-human IgG/IgM antibody is conjugated with an enzyme or fluorescent tag that reports signals. For ELISA, horseradish peroxidase (HRP) is used for catalyzing the conversion of chromogenic substrates tetramethylbenzidine (TMB) to produce a color change quantifiable by optical absorbance. Similarly, the enzyme, e.g., HRP or alkaline phosphatase (ALP), can be also used in CLIA to catalyze the light emission of the chemiluminescent substrate. However, different from ELISA where the multi-well plate is used as the substrate for immunoaffinity binding, in CLIA, the SARS-CoV-2 antigen is mostly immobilized on magnetic

particles to facilitate the removal of non-binding enzymes and automate the process. On the other hand, FIA relies on the labeling of the fluorophore on the binding agent to report signals. It can be versatile in different platforms and formats, but a specific fluorescence analyzer is needed. Finally, in contrast to the detection methods above, LFIA uses immunochromatography to provide a color band as a reporter. Generally, gold nanoparticles are conjugated with the SARS-CoV-2 antigen and mixed with the serum sample at the sample pad. Carried by a capillary flow in a cellulose membrane, the gold particles with the captured target IgG/IgM antibody would be captured and immobilized at separate lines precoated with the anti-human IgG/IgM antibody. Therefore, their accumulation generates a color band available for visual inspection.

The major difference between these methods is clear. The ELISA and FIA are the most popular methods for quantitative analysis and have been considered the gold standard of an immunoassay for antibody detection. However, they are labor intensive since multiple rinsing steps are required to remove unbound antigens and antibodies. In contrast, the CLIA provides a high degree of automation and the possibility of handling a large number of samples simultaneously. However, they heavily rely on complex machinery and laboratory skills, which are only available in professional clinics or laboratories. On the other hand, the LFIA provides a unique alternative with visible results on a simple, cost-effective, and portable platform, making it particularly suitable for untrained end-users. However, the lateral flow method relies on the appearance of color bands, which are mostly for yes/no signals and hard to quantify, as seen in Fig. 1(b). Such a limitation makes the result difficult to interpret and ambiguous. A systematic comparison conducted by Kontou *et al.* have confirmed that while ELISA and CLIA provide sensitivity over 90%, the sensitivity of LFIA can only reach 53% to 66%.²² Thus, the ELISA and CLIA tests will be suitable for more precise and accurate detections, while LFIA tests are particularly useful for the large-scale surveillance of serological immunity with the lower requirement of sensitivity.

IV. MICROFLUIDIC IMMUNOASSAY FOR ANTIBODY DETECTION

Due to overwhelmed medical facilities, there are demands for miniaturized tests that are simple and can be performed at home by non-medical personnel. However, to achieve meaningful detection, the antibody test should be (1) sensitive, to prevent false-negatives, (2) quantitative, to allow clear-cut evaluation of immunity without ambiguity, and (3) suitable for point-of-care testing, for conducting large-scale surveillance without increasing medical burden. While LFIA's portability and easy-to-use format make it a good candidate, the insufficient sensitivity and qualitative readout are the main obstacles in obtaining significant and meaningful results for diagnosis.

Due to such demands, microfluidics has attracted much attention in recent decades because it enables low reagent consumption, high throughput, and rapid analysis. The first attempt of microfluidic ELISA for antibody detection was demonstrated by Eteshola and Leckband, who achieved a limit of detection of 17 nM on the detection of rabbit anti-sheep IgM antibodies.²⁹ Later, other attempts were made to miniaturize the ELISA,^{30,31} CLIA,^{32–34} and FIA^{30,31,35,36} into microfluidic platforms. Notably, such a platform has not only achieved good sensitivity and detection limits comparable to conventional ELISA but also greatly save the analysis time, requirement sample size, and reagent. In what follows, we discuss and compare the progress achieved using microfluidic-based immunoassays for antibody detections through different aspects including surface modification, microfluidic kinetics, signal output, signal amplification, and sample matrix. Notably, the microfluidic-based immunoassays selected for comparison are not only for antibodies against viral infection but also for other pathogens or disease models since the same principle can also be applied to SARS-CoV-2 antibodies. Finally, we report two very recent articles

using microfluidic immunoassay for the detection of anti-SARS-CoV-2 antibodies.

A. Surface modifications

Appropriate surface modification is the first technical challenge for achieving microfluidic immunoassay. Due to the excessive denaturation of proteins caused by hydrophobic interactions through the conventional surface adsorption of antibodies, the treatment of the surface to maintain the protein function is crucial. Generally, the microfluidics platform is based on microchannels fabricated using silicon,³³ poly(dimethylsiloxane) (PDMS),^{29,31,32,35,37,38} and poly(methyl methacrylate) (PMMA)^{36,39} as the common materials. However, without special treatment, the protein adsorption on those materials is limited, which prevents protein immobilization and immunoaffinity binding for successful immunoassay. In the past decades, the effort has been spent to investigate a suitable surface treatment enhancing antibody binding. For example, Bai *et al.*³⁶ study the surface treatment using amine bearing compounds [Fig. 2(a)]. Amine bearing molecules such as polyethylenimine (PEI) and PAH [poly(allylamine hydrochloride)] show a fluorescence reaction rate (RFU/s) of 16 RFU/s and 14 RFU/s, respectively, which is 16 times better than the non-treated PMMA surface. In addition, Wen *et al.*³⁹ utilize amine bearing polymer PLL [poly(l-lysine)] complex forming a biotin-PLL-g-PEG graft copolymer alongside protein A to treat a PMMA surface [Fig. 2(b)]. Here, the copolymer complex and protein A functions as a tool to improve the antibody capture efficiency and conform to antibodies orientation. On the silica surface, PEI was used to enhance antibody immobilization. However, instead of physical adsorption, the covalent coupling of antibodies via glutaraldehyde is required to stabilize them.³³ Comparative study illustrates the performance of the utilization of the copolymer complex, where the combination of plasma treated PAA-biotin-PLL-g-PEG-Protein A can yield a fluorescence reaction rate up to 53 RFU/s compared to the 1.40 RFU/s for the PEI treated PMMA discussed previously [Fig. 2(c)].³⁹

On the other hand, the PDMS surface has been reported with high hydrophobicity and avidity, which makes the passive adsorption of the antibody/protein ineffective.²⁹ To address it, the PDMS surface was either plasma treated with varied duration³⁵ or activated by UV-ozone³¹ to enhance the protein adsorption. Moreover, the buffer solution for blocking was also optimized to minimize non-specific bindings and background noise.^{29,35} However, while physical adsorption is convenient to immobilize large amounts of protein, effective blocking has been difficult. Thus, selective immobilization using protein A has been applied to PDMS microchannels.²⁹ After uniformly coating of BSA, the BSA was activated by glutaraldehyde, which enables covalent binding of protein A via the glutaraldehyde groups similar to the modification on PMMA surface.³³ In such selective immobilization, the signal to noise ratio can be improved up to five times.²⁹

Glass is also a common material used for microfluidic devices. Cleaned glass was used for the deposition of assays of protein spots. After drying, PDMS precursor was poured and cured onto it, allowing the protein spots being transferred to the PDMS surface after being peeled off. Using this pattern transfer, the complicated procedure of the surface treatment is greatly simplified.³² Also,

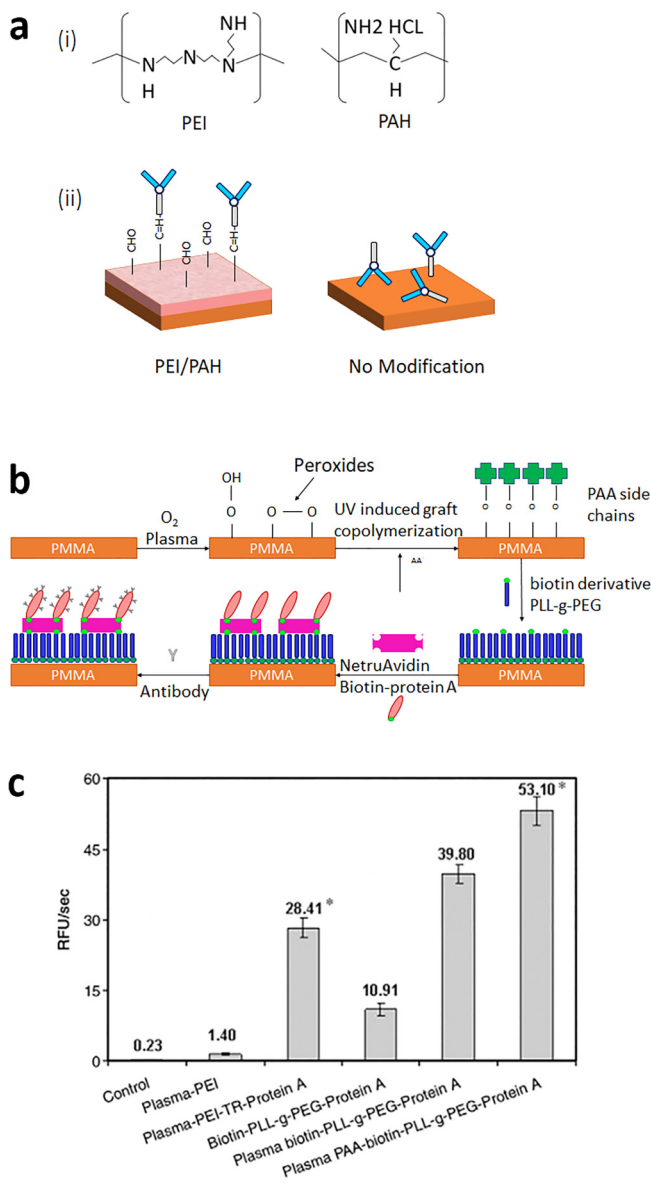


FIG. 2. Surface treatment on substrate with (a) (i) PEI and PAH chemical structure. (ii) Illustration of the spatial effects of different surface modification on antibody binding on the PMMA surface of surfaces treated with PEI or PAH (left) and passive adsorption of antibodies on PMMA surface without modification, which could result in disorientation and functional disability upon binding (right). (b) Biotin-PLL-g-PEG protein A-based antibody immobilization schematic.³⁹ (c) Compared immunoassay performance between different surface treatments for the detection of anti-INF- γ .³⁹ (b) and (c) Reprinted with permission from Wen et al., J. Immunol. Methods **350**(1–2), 97–105 (2009). Copyright 2009 Elsevier.

after coated with aminosilane, the glass surface can also bind to protein A and G for immobilizing the capture antibodies.³⁴ To ensure the original conformation of the immobilized protein, Cretich *et al.* synthesized another copolymer combining N,

N-dimethylacrylamide (DMA) and N,N-acryloyloxy succinimide (NAS) by grafting it to a glass surface.⁴⁰ The surface is first coated with MPS (3-mercaptopropyl silane) through silanization, followed by DMA and NAS coating. Through polymerization, DMA and NAS would form a copolymer binding to the MPS, forming a brush-like structure with a free NAS amine group which could be modified to fulfill specific requirements. Through this copolymer treatment, antibodies can be immobilized with their native conformation. Moreover, they also provide low fluorescence background, which allows the usage of high laser power (90%) and dial-up the PMT (Photomultiplier Tube Sensitivity) to 90% enhancing the sensitivity of the assay with a threefold to fivefold IgE reactivity.

B. Microfluidic kinetics

It is, in fact, non-trivial to accomplish multiple rinsing steps in a miniaturized immunoassay. Pressure-driven flow carried out by a syringe pump or peristaltic pump for reagent loading and rising are mostly used for protein immobilization and antibody binding.²⁹⁻³³ While it is the most convenient approach, the integration between the microfluidics platform and the pump makes the device bulky and complicate to operate. To address it, electrokinetic-driven flow has been proposed,³⁵ which enables easy integration of pumping mechanism and automates flow control for microfluidic immunoassay. However, the electrokinetic mobility is highly dependent on the buffer solution and the zeta potential of the channel wall,³⁵ which may restrict the suitable buffer environment and blocking agent. To completely avoid the immobilization and washing, researchers proposed the use of microchannels for capillary electrophoresis, which can effectively separate the immune complex from free antibody or antigen based on the difference of charge-to-mass ratios. In this way, the detection of the antibody can be achieved by a newly appeared fluorescent peak representing the antibody–antigen complex. Such capillary electrophoresis can be used for the direct quantification of a specific antibody, e.g., tetanus antibodies.⁴¹ When combining with online mass spectrometry, it can even discriminate monoclonal antibody variants.⁴²

Microfluidic kinetics can be also used for enhancing antibody-antigen binding. Immunoassays are often mass transport limited since molecules' interaction is usually confined on the surface of microchannels.⁴³ Thus, when the solution is introduced, a large number of molecules might pass by the reaction zone without effective binding. Overcoming this binding efficiency can be optimized through the mixing at the reaction zone of the microfluidic device. Cretich *et al.* enhanced the detection sensitivity of allergen specific IgE by integrating microarray in a microflow cell, which allows dynamic incubation of serum [Fig. 3(a)].⁴⁰ With the aid of sequential insertion of reagents from multiple reservoirs, this automated flow facilitated the amalgamation of the antibody with their respective allergen, hence eliminating the mass transport limit. Comparing the conventional 2-h static incubation protocol, this microfluidic assay with 10 min of dynamic incubation showed improvement of IgE fluorescence signals up to six times.⁴⁰ Similarly, Singhal *et al.* designed a microfluidic device with control valves to control the association and dissociation rate of the binding interaction [Fig. 3(b)].³⁷ With this setup, they can achieve 8×10^4 antibody molecules (132 zeptomoles) immobilized on a

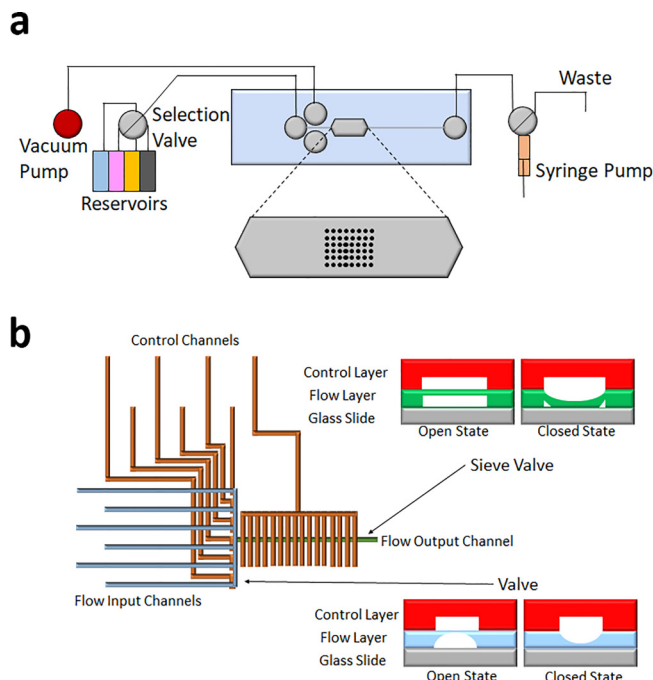


FIG. 3. Microfluidic device schemes with kinetic facilitation. (a) Device scheme connected to a software-controlled selector valve and syringe pump which sequentially introduce reagents from the reservoirs.⁴⁰ Reprinted with permission from Chiari *et al.*, *Proteomics*, **9**/**8**, 2098–2107 (2009). Copyright 2009 John Wiley and Sons. (b) Device schematic utilizing control channels (orange) and sieve valves on the outlet reagent channel (green), which controls the interaction of fluids inside the microfluidic system.³⁷ Reprinted with permission from Singhal *et al.*, *Anal. Chem.* **82**/**20**, 8671–8679 (2010). Copyright 2010 American Chemical Society.

single bead with less than 2×10^6 antibodies injected into the system.

C. Signal output

The signal acquisition on the microfluidic platform is also a concern. Traditionally, the fluorescence and chemiluminescence signals are acquired and analyzed by a microscope with a image detector, e.g., a CCD camera or a photomultiplier tube,^{32,33,35,36} which make the entire system impractical for miniaturized tests (Fig. 4). Some other more advanced optical systems were also used but require even more sophisticated optical setups.^{43,58} To miniaturize the detection module, there are attempts such as using integrated photodiodes onto the microchannels at the test zone, while light sources such as LED or laser were used for the measurement of optical absorbance.^{30,31} However, the alignment of the light source, test zone, and photodiodes is essential for accurate measurement, which requires special care during the design process. To ease the optical setting, it has been reported that immunobinding on the channel wall would change the long-range orientation of the liquid crystal above it, resulting in a bright optical signal observable

by the naked eye or under a polarized microscope.^{44,45} More importantly, by flowing antibodies along the microchannels uniformly coated with antigen, the concentration of antibodies would reflect a changed length of the bright region due to the difference of the binding rate and characteristic binding time,⁴⁴ allowing quantitative signal readout.

On the other hand, to avoid the use of optical systems, the electrochemical reaction has become an easier approach for data acquisition on microfluidic platforms (Fig. 4).^{41,46–48} The key of electrochemical detection is to use enzymes labeled on the detection antibodies to convert the binding event into an amperometric output. The common enzymes of use are HRP and ALP. By catalyzing a redox reaction, substrates such as p-aminophenyl phosphate (PPAP) and tetramethylbenzidine (TMB) are oxidized, and the exchanged electrons can then be used for generating an amperometric current. Comparing to the measurement of optical signals, amperometric current can be quantitatively measured by electrodes, which is a much more sensitive, low-cost, and easy-to-use platform. For example, Zhao and Lin have developed paper-based microfluidic platform allowing the multiplexed detection of human immunodeficiency virus (HIV) and hepatitis C virus (HCV) antibodies in serum samples.⁴⁸ They have achieved LOD of 300 pg/ml and 750 pg/ml, which is much better than the ELISA-based microfluidic platform for HIV antibodies ($10\text{--}22 \times 10^{10}$ pg/ml).³⁰ Since only electronic components are used, the material cost of the amperometric meter can be as low as CAD \$60,⁴⁸ providing a great advantage of device miniaturization.

D. Micro/nanoparticles conjugates for signal amplification

A limitation of microfluidic immunoassays is the finite area of contact used to immobilize biological agents. Traditional immunoassays usually are done on a flat surface, which only has a two-dimensional functional area to capture antibodies. To increase the effective immobilization region, micro/nanoparticles have been utilized due to their high surface area that promotes more antibody capture, which amplifies the signal generated by the assay [Fig. 5(a)]. Utilization of these microbeads can be done through various means. One approach commonly used is by utilizing magnetic/paramagnetic beads for a better localization with the use of an external magnetic field. Pereira *et al.*⁴⁹ use magnetic microbeads coupled with a gold electrode in a microfluidic channel to capture the antibodies of bacteria *H. pylori* that causes chronic digestive issues. Their work can achieve a limit of detection of 0.37 U/ml compared to 2.1 U/ml of the traditional ELISA procedure in a total assay time of 25 min. Similarly, Lee *et al.* utilize epoxy coated magnetic microbeads to capture dengue virus antibodies with a detection limit of 21 pg/ml [Fig. 5(b)].⁵⁰ Usage of gold nanoparticles (AuNPs) is very popular in the field of electrochemical immunoassays due to their versatile properties and great surface-to-volume ratio, which enhance the biomolecule binding site and the sensitivity of the devices. Studies by Pereira *et al.* utilize gold nanoparticles to modify surfaces to different electrode materials for specific antibody immobilization. Gold nanoparticles deposited electrochemically to the electrode surface are primarily dictated by certain parameters such as the time of deposition (*t_{dep}*) and the deposition

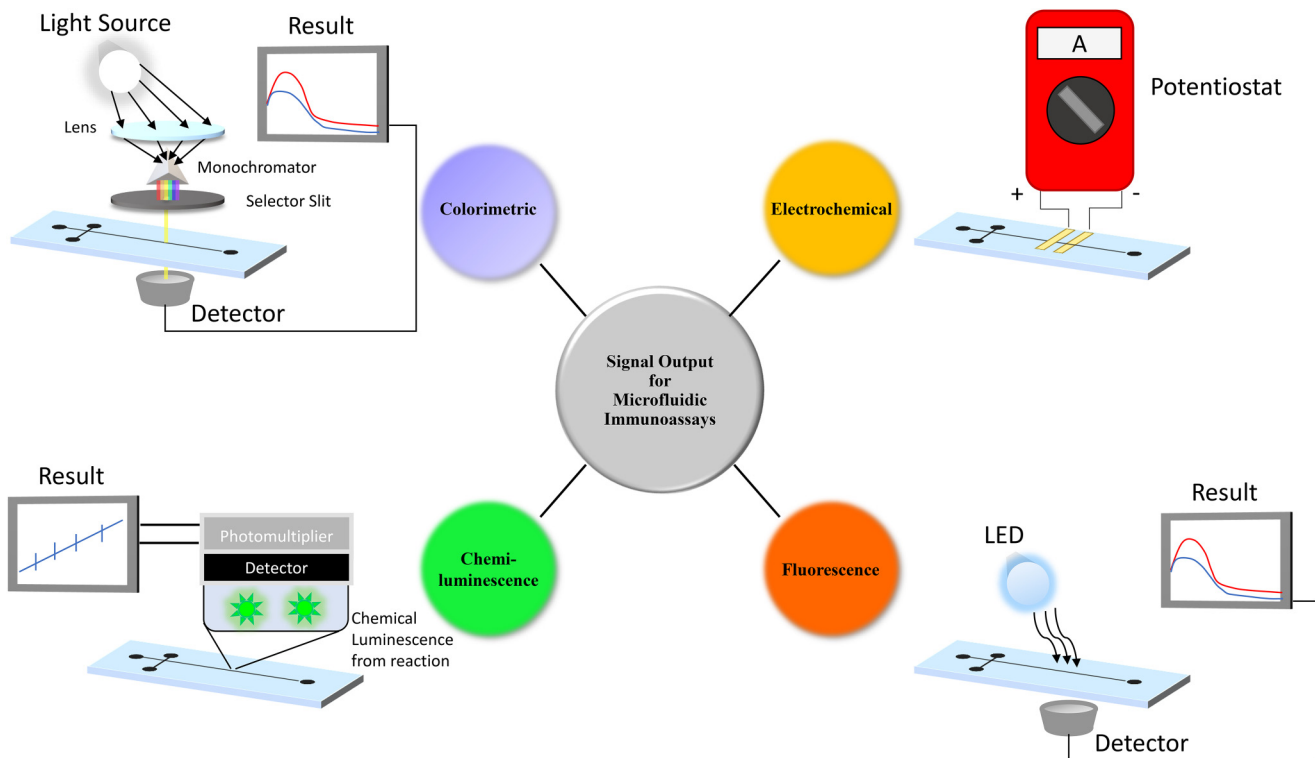


FIG. 4. Signal acquisition on microfluidic immunoassays with their common detection methods.

potential (E_{dep}). After optimizing the electrochemical deposition of gold nanoparticles, Pereira *et al.*⁵¹ achieved a limit of detection of 3.065 ng/ml and an inter-assay variation of 6.95% for the detection of anti-*Trypanosoma cruzi* antibodies. Another study by Pereira⁵² modified the gold electrode with the 1,6-hexanedithiol (1,6-HDT) solution forming a self-assembled monolayer (SAM) atop the gold electrode surface. The 1,6-HDT solution modified gold electrode was then exposed to the gold nanoparticles and then reacted with mercaptopropionic acid containing –SH groups. Here, the reaction between the acid and the surface of the gold nanoparticles will produce free COOH groups that will promote the antigen binding of the target antibody [Fig. 5(c)]. When applied to the detection of antibodies of *Echinococcus granulosus*, a limit of detection of 0.091 ng/ml with 6.7% inter-assay variation within 26 min was achieved, which is much less than conventional immunoassays.

E. Sample matrix

The ability to handle the sample matrix is also very crucial. A common form of the sample matrix used in the detection of antibodies is either serum or whole blood. Serum-based microfluidic immunoassays separate the blood serum from the whole blood prior to the insertion of the microfluidic device through centrifugation.^{32,40,49–54} Through it, the wanted biomolecule could be isolated to improve performance of the device.³⁰ Whole blood matrices give extra advantages of allowing multiplex detection due

to the presence of a wide range of biomolecules.⁵⁵ Example of these separation methods are centrifugation through a lab-on-a-disk approach⁵⁶ and filtration in the lateral flow immunoassays.⁵⁵ With such addition of the separation mechanism, microfluidic immunoassays could provide an insignificant difference in detection performance from its serum-based counterpart.

F. Application to detection in anti-SARS-CoV-2 antibodies

In the battle against COVID-19, some microfluidic approaches for the antibody detection of the SARS-CoV-2 have recently emerged. One device was fabricated by Swank *et al.*⁵⁷ with a MITOMI (Mechanically Induced Trapping of Molecular Interaction). In this method, the presence of anti-SARS-CoV-2 would be captured by immobilized SARS-CoV-2 spike protein and report fluorescence signals upon binding to an anti-human IgG antibody conjugated with phycoerythrin. With the aid of automated flow control on 1024-unit reaction chambers on a microfluidic platform, high-throughput analysis was enabled. The limit of detection is around 1 nM of IgG. Applying to total 289 serum samples, i.e., a sample of 155 people tested positive for SARS-CoV-2 and 134 negatively tested, 100% specificity and 98% sensitivity were achieved, which they claimed to be as good or better than standard ELISA. On the other hand, another device fabricated by Funari *et al.*⁵⁸ utilize gold nanospikes in label-free

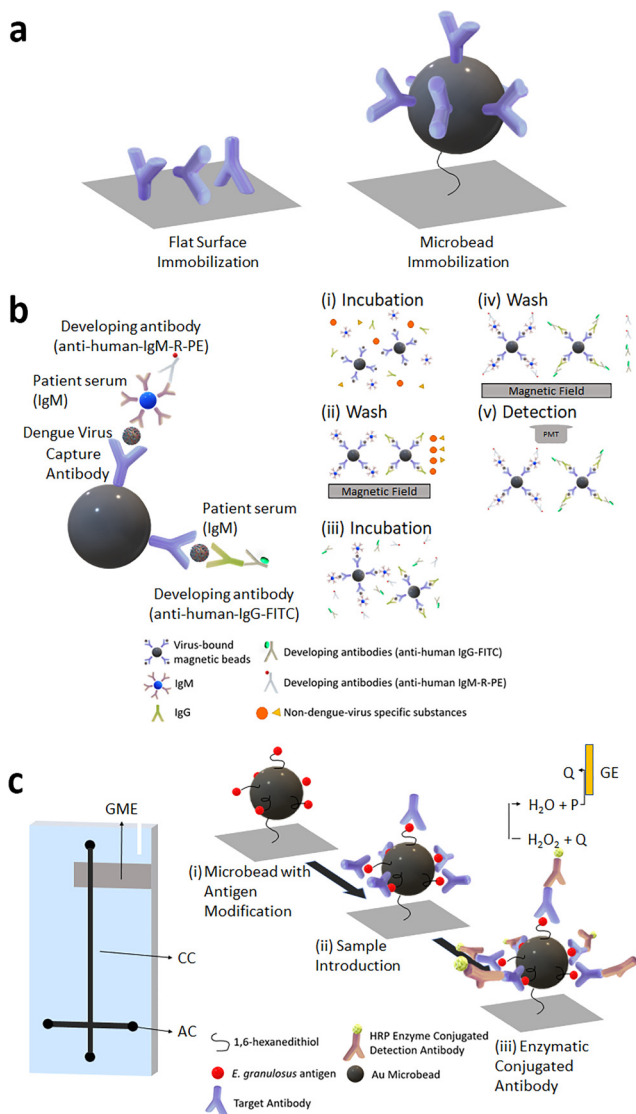


FIG. 5. (a) Illustration of the advantage of microbead conjugation in microfluidic immunoassays, which provides the larger surface area for antibody immobilization. (b) Illustration of a sandwich-based immunoassay with magnetic beads for human anti-dengue antibody (left) and steps for the detection of human anti-dengue virus IgG/IgM by using virus-bound magnetic beads in the microfluidic system.⁵⁰ Reprinted Lee *et al.* from Biosens. Bioelectron. **25**/**4**, 745–752 (2009). Copyright 2009 Elsevier. (c) Schematic representation of the immunomicrofluidic device (GME, modified gold electrode; CC, central channel; AC, accessory channel) and the immune and enzymatic reactions of the system.⁵² Reprinted from Pereira *et al.* Anal. Biochem. **409**/**1**, 98–104 (2011). Copyright 2011 Elsevier.

opto-microfluidic sensing to detect SARS-CoV-2 spike protein antibodies in human plasma. By measuring the wavelength shift of the localized surface plasmon resonance caused by the local refractive index change when anti-SARS-CoV-2 antibodies bind to the

surface, this device achieved a limit of detection of approximately 0.08 ng/ml, which falls under the clinical detection range.

V. SUMMARY AND FUTURE PERSPECTIVES

Due to the recent pandemic of COVID-19, millions of people's lives have been affected because of mandatory isolations/quarantines, which hamstring economies and causing fears and panic. To resume normal life, there is an increasing demand for the IgG/IgM antibody test so that people can be more conscious and document their immune status, which is required before resuming work, flight travel, border entry control, and to speed up the recovery from pandemic's catastrophic damage on the global economy. In addition, if widely accepted, it would also provide the level of herd immunity for public policymakers, especially the percentage of asymptomatic and immured cases in a population. Moreover, it can also be used to evaluate the efficacy of vaccines during clinical trials, which is crucial to save lives and bring back normality.

Conventionally, ELISA, FIA, and CLIA are reliable methods with quantitative readouts, but they also require sophisticated equipments, labor-intensive protocols, and profession operators, which are not accessible by ordinary end-users. On the other hand, the LFIA uses the appearance of a color band as the signal readout similar to the pregnancy test, providing a unique advantage with visual results using a simple, cost-effective, and portable platform. However, it is only for yes/no signals by visual inspection, and quantitative measurement can only be obtained through a special strip reader. As a result, it is difficult to achieve simple and portable platforms as cumbersome, bulky instruments are still inevitable. In fact, many LFIA kits were reported only to be able to identify immunity accurately in people who had been severely ill.

In the past decades, many portable sensors with visual signals have been reported. In this Review, we summarize the detection of antibodies on microfluidic platforms (Table I), including but not limited to antibodies against viral infections. Different methods have been grouped together based on their signal output to compare the performances of each microfluidic device. Among all the methods reviewed, the limit of detection (LOD) of most microfluidic detection ranges from 0.01 to 30 000 ng/ml with fluorescence, chemiluminescence, and colorimetry format, depending on the detection strategy and the use of signal amplification. Moreover, to achieve the quantitative measurement with sufficient sensitivity, optical setups are required, which is impractical and even more difficult to implement on miniaturized devices. In contrast, electrochemical based microfluidic assays can detect biomolecules as low as 0.003 ng/ml⁴⁷ and 0.091 ng/ml, respectively, indicating the superior sensitivity of the electrochemical detection. However, rinsing/washing steps are still needed, which makes the automated pumping inevitable. Furthermore, dilution and removal of IgG are usually required if the sample matrix is a serum or the whole blood.^{30,34,40,41,47–49,51,55}

Apparently, the current development of microfluidic immunoassays is still restricted to laboratory-based detection. While good detection performance is achieved, challenges are still faced for applications to untrained end-users. To conduct large-scale surveillance, it is indeed important to maintain the advantage such as portability, simple-to-use, no requirement of equipment, and low

TABLE I. Summary of microfluidic approaches for the antibody detection based on their signal output.

Method	Antibody	LOD (ng/ml)	Detection range (ng/ml)	Signal output	Sample matrix	Modification	Sample-result time (min)	Disease application	Reference
Chemiluminescence									
Microfluidic biochip	Anti-human IgG antibodies	9.9 ^a	9.9–495	Chemiluminescence	Carbonate buffer or serum		6	Allergy diagnostic	32
Microspot ELISA	Anti-mouse IgG	0.182 pmol/cm ²	0–4.995 × 10 ⁵	Chemiluminescence	PBS buffer		30		31
Silicon microchip	Polyclonal anti- atrazine IgG	0.045, 0.038, 8×10^4		Chemiluminescence			10		33
Microfluidic LIPS	Anti-HSV2 antibodies								
Colorimetric	FITC-anti-IgG and FITC-anti-biotin antibody	2.0 × 10 ⁴	2–8 × 10 ⁴	Colorimetric	PBS buffer		130		44
Liquid crystals	Anti-rabbit IgG	1000	100–1 × 10 ⁴	Colorimetric	PBS buffer		25	Malaria and Salmonella	45
Multiplex card microfluidic immunoassay	Anti- <i>Salmonella typhi</i> LPS IgG	10–20	0–100	Colorimetric	Whole blood			Hepatitis B	55
Lab on a disk immunoassay	Anti-hepatitis B antibody	691.4 ^b	0–8.04 × 10 ⁴	Colorimetric	Whole blood		30		56
Smartphone dongle	HIV rabbit anti-goat IgG antibody			Colorimetric	Lysed whole blood			Haemoglobin concentration related diseases	30
								HIV syphilis	
Fluorescence									
ELISA in PDMS microfluidic channels	Rabbit anti-sheep IgM	1.53 × 10 ⁴	0–35	Fluorescence	PBS + BSA + Tween	Kinetics			29
Antigen-antibody kinetics binding microfluidic ELISA	Rabbit anti-mouse polyclonal antibodies (pAbs) Anti-IFN-γ IgG	8 × 10 ⁴		Fluorescence	PBS buffer	Surface treatment			37
Specific antibody immobilization treatment									
microfluidic ELISA	Anti- <i>H-pylori</i> human IgG	1000	10 ³ –10 ⁵	Fluorescence	TBS buffer		30	Gastritis, peptic ulcer disease and gastric cancers	35
Electrokinetic microfluidic immunoassay									

TABLE I. (Continued.)

Method	Antibody	LOD (ng/ml)	Detection range (ng/ml)	Signal output	Sample matrix	Modification	Sample-result time (min)	Disease application	Reference
Surface modification on microfluidic ELISA	Rat IgG	5–1000	Fluorescence	PBS buffer	PEI treated surface	241			36
Magnetic microbeads	Dengue virus IgG	0.21	0.109–450	Fluorescence	Serum	Magnetic microbeads	30	Dengue fever	50
Quantitative microfluidic droplet array	Diabetes antibodies targeting insulin, GAD, and IA-2	0.0196, 0.0187, 0.0127	0.05–1, 0.1–1	Fluorescence	Hydrogel		120	Diabetes	38
Microarray microfluidic ELISA	Allergen specific IgE	9.6 ^b		Fluorescence	Serum	Surface treatment + kinetics	25	IgE allergens	40
Laser induced fluorescence	Anti- <i>Helicobacter pylori</i> human IgG	1.37 × 10 ^{4b}	0–8.04 × 10 ⁷	Fluorescence	Serum	Laser induced fluorescence	28	Gastritis, peptic ulcer, gastric adenocarcinoma, and mucosa associated lymphoid tissue lymphoma SARS-CoV-2	54
Microfluidic nano-immunoassay	Anti-SARS-CoV-2 IgG	150 ^a	0–15000	Fluorescence	Whole blood		>60		57
Other optics									
Antibody-surface binding kinetics ELISA	Anti-rabbit IgG	70 ng/cm ²		Ellipsometry	Serum	Kinetics			43
Gold nanospike opto-microfluidic chip	Anti-SARS-CoV-2 spike protein IgG	0.08	1–100	Surface plasmon resonance	Serum		30		58
Electrochemical carbon electrode with electrodeposited gold nanoparticles immunosensor	Anti- <i>Trypanosoma cruzi</i> antibodies human IgG	3.065	11–205	Electrochemical	Serum	Gold nanoparticles	26	Chagas disease	51
Paper-based microfluidic immunosensor	Antibodies against HIV p24 core antigen and HCV core antigen	0.3 and 0.75	0–10 ⁴	Electrochemical	Serum		20	HIV and hepatitis C	48
Electrochemical immunoensor on TES-AuNP and CMK-8	Anti- <i>Toxocara canis</i> human IgG	0.1	0.1–100	Electrochemical	Serum	Gold nanoparticles	20	Toxocariasis	53
Gold nanoparticle immunoensor	Anti- <i>Echinococcus granulosus</i> human IgG	0.091	0.5–115	Electrochemical	Serum	1,6 HDT gold nanoparticles	26	Hydatidosis	52
Electrochemical immunoensor	Aminoterinal pro-brain natriuretic peptides (NT-proBNP)	0.003	0–4	Electrochemical	Whole blood		>18	Heart failure	47

Microfluidic magnetic immunoassay	Anti- <i>Helicobacter pylori</i> human IgG	2.9748 × 10 ⁻⁶	0–8.04 × 10 ⁻⁶	Electrochemical	Serum	Magnetic Microbeads	25	Chronic active type B gastritis and peptic ulcer diseases	49
Electrophoresis									41
Gel-electrophoresis immunoassay	Anti-tetanus human IgG	25.5 ^a	25.5–3.9 × 10 ³	Electrophoresis	Serum		3	Tetanus	42
Capillary electrophoresis-electrospray				Electrophoresis	2-Propanol/ acetic acid				42

^aLOD calculated by assuming IgG, IgE molecular weight as 150 kDa and IgM molecular weight as 900 kDa.

^bLOD converted from IU/ml to ng/ml by using the estimated conversion factor: IgG: 80.4 μg/IU, IgA: 14.2 μg/IU, IgE: 0.0024 μg/IU, and IgM 8.47 μg/IU.

cost. Moreover, to prevent false diagnosis, it is also expected to achieve (1) sufficient sensitivity, (2) quantitative measurement preferably by visual inspection without relying on complicated equipment, and (3) better compatibility with the whole blood, which is particularly suitable for home-use since centrifuge is unlikely available at home.

In fact, there are attempts based on the appearance of a visible bar on the accumulation of nanoparticles in the microchannels for visual detections.⁵⁹ In particular, quantitative measurements were also allowed by the movement of an ink bar^{60–62} or microparticle accumulation in a microfluidic chip.⁶³ Among them, ELISA-based immunoassay has been demonstrated with the visual quantitative result.⁶² Here, instead of directly measuring the change of solution color, as that in the immunosorbent assay, this work utilizes catalyze to react with hydrogen peroxide to produce and release oxygen gas to push preloaded inked bars. Thus, because the channels are in the microscale geometry, the movement of the ink bar becomes visible and quantitative, which is superior to all the other signal acquisition methods. On the other hand, combining microparticles and microfluidic platforms, our group has also developed a simple and sensitive microfluidic particle dam enabling visual quantification of oligonucleotide and lead ion by the naked eye.^{63–65} Here, similar to the immunoaffinity binding, the present linker molecules, e.g., DNA oligonucleotide or lead-dependent DNAzyme, were used to connect magnetic microparticles (MMPs) and polystyrene microparticles (PMPs), forming “MMPs-linker-PMPs.” Thus, the amount of linker would be proportional to the connections between MMPs and PMPs. To quantify it, the solution is loaded to a capillary-driven microfluidic device where MMPs and the MMPs-linker-PMPs are first removed by a magnetic separator, leaving the free PMPs continuing to flow until being trapped and accumulate at a particle dam. Thus, the PMP accumulation eventually forms a visual bar quantifiable by the length. Together, while the current microfluidic immunoassays offer advantages of saving the analysis time and reduction of sample size and reagent, the direct miniaturization of the conventional immunoassays onto a microfluidic platform has made the device integration difficult and impractical. Instead, those visual quantitative methods truly utilize the advantage of microscale channels to display the quantitative signal readable with the naked eye, suggesting a new perspective for the future development of microfluidic immunoassays.

In summary, the mandatory isolations/quarantines due to the pandemic of COVID-19 have raised increasing interest in antibody detection. However, instead of directly miniaturizing the conventional immunoassays onto the microfluidic platform, new approaches using visual quantitative signals may provide a new concept to cope with the detection of viral immunity in views of the current COVID-19 pandemic. Thus, such detection is envisioned to be applied for the detection of viral immunity, allowing the determination of the actual level of immunity to COVID-19 for point-of-care testing, to relax the burden on the healthcare system, and to accelerate the recovery of economic damages.

ACKNOWLEDGMENTS

We are pleased to acknowledge the funding support from the City University of Hong Kong (No. 6000720) and the Research

Grant Council, University Grants Committee (Nos. N_CityU119/19, 11217217, 11277516, and 11217820).

DATA AVAILABILITY

The data that support the findings of this study are available within the article.

REFERENCES

- ¹T. P. Sheahan *et al.*, “Comparative therapeutic efficacy of remdesivir and combination lopinavir, ritonavir, and interferon beta against MERS-CoV,” *Nat. Commun.* **11**(1), 222 (2020).
- ²S. Su *et al.*, “Epidemiology, genetic recombination, and pathogenesis of coronaviruses,” *Trends Microbiol.* **24**(6), 490–502 (2016).
- ³N. Zhu *et al.*, “A novel coronavirus from patients with pneumonia in China, 2019,” *N. Engl. J. Med.* **382**(8), 727–733 (2020).
- ⁴E. Petersen *et al.*, “Comparing SARS-CoV-2 with SARS-CoV and influenza pandemics,” *Lancet Infect. Dis.* **20**(9), 238–244 (2020).
- ⁵J. F.-W. Chan *et al.*, “A familial cluster of pneumonia associated with the 2019 novel coronavirus indicating person-to-person transmission: A study of a family cluster,” *Lancet* **395**(10223), 514–523 (2020).
- ⁶N. Dong *et al.*, “Genomic and protein structure modelling analysis depicts the origin and infectivity of 2019-nCoV, a new coronavirus which caused a pneumonia outbreak in Wuhan, China,” *biorxiv* (2020).
- ⁷S. A. Lauer *et al.*, “The incubation period of coronavirus disease 2019 (COVID-19) from publicly reported confirmed cases: Estimation and application,” *Ann. Intern. Med.* **172**(9), 577–582 (2020).
- ⁸K. K.-W. To *et al.*, “Temporal profiles of viral load in posterior oropharyngeal saliva samples and serum antibody responses during infection by SARS-CoV-2: An observational cohort study,” *Lancet Infect. Dis.* **20**(5), 565–574 (2020).
- ⁹M. Z. Shen *et al.*, “Recent advances and perspectives of nucleic acid detection for coronavirus,” *J. Pharm. Anal.* **10**(2), 97–101 (2020).
- ¹⁰C. Liu *et al.*, “Research and development on therapeutic agents and vaccines for COVID-19 and related human coronavirus diseases,” *ACS Cent. Sci.* **6**(3), 315–331 (2020).
- ¹¹M. Wang *et al.*, “Remdesivir and chloroquine effectively inhibit the recently emerged novel coronavirus (2019-nCoV) in vitro,” *Cell Res.* **30**(3), 269–271 (2020).
- ¹²R. Lu *et al.*, “Genomic characterisation and epidemiology of 2019 novel coronavirus: Implications for virus origins and receptor binding,” *Lancet* **395**(10224), 565–574 (2020).
- ¹³P. Zhou *et al.*, “Fatal swine acute diarrhoea syndrome caused by an HKU2-related coronavirus of bat origin,” *Nature* **556**(7700), 255–258 (2018).
- ¹⁴D. Wrapp, N. Wang, K. S. Corbett, J. A. Goldsmith, C.-L. Hsieh, O. Abiona, B. S. Graham, and J. S. McLellan, “Cryo-EM structure of the 2019-nCoV spike in the prefusion conformation,” *Science* **367**(6483), 1260–1263 (2020).
- ¹⁵L. Du *et al.*, “The spike protein of SARS-CoV—A target for vaccine and therapeutic development,” *Nat. Rev. Microbiol.* **7**(3), 226–236 (2009).
- ¹⁶M. Hoffmann *et al.*, “SARS-CoV-2 cell entry depends on ACE2 and TMPRSS2 and is blocked by a clinically proven protease inhibitor,” *Cell* **181**(2), 271–280 (2020).
- ¹⁷M. A. French and Y. Moodley, “The role of SARS-CoV-2 antibodies in COVID-19: Healing in most, harm at times,” *Respirology* **25**(7), 680–682 (2020).
- ¹⁸X. Liua *et al.*, “Patterns of IgG and IgM antibody response in COVID-19 patients,” *Emerg. Microbes Infect.* **9**(1), 1269–1274 (2020).
- ¹⁹A. Longchamp *et al.*, “Serum antibody response in critically ill patients with COVID-19,” *Intensive Care Med.* **46**(10), 1921–1923 (2020).
- ²⁰A. Petherick, “Developing antibody tests for SARS-CoV-2,” *Lancet* **395**(10230), P1101–P1102 (2020).
- ²¹S. K. Law, A. W. Leung, and C. Xu, “Is reinfection possible after recovery from COVID-19?,” *Hong Kong Med. J.* **26**(3), 264–265 (2020).
- ²²P. I. Kontou *et al.*, “Antibody tests in detecting SARS-CoV-2 infection: A meta-analysis,” *Diagnostics* **10**(5), 319 (2020).
- ²³F. Wolff *et al.*, “Monitoring antibody response following SARS-CoV-2 infection: Diagnostic efficiency of four automated immunoassays,” *Diagn. Microbiol. Infect. Dis.* **98**(3), 115140 (2020).
- ²⁴Y. Wu, “Compensation of ACE2 function for possible clinical management of 2019-nCoV-induced acute lung injury,” *Virol. Sin.* **35**(3), 256–258 (2020).
- ²⁵H. B. Lv *et al.*, “Cross-reactive antibody response between SARS-CoV-2 and SARS-CoV infections,” *Cell Rep.* **31**(9), 107725 (2020).
- ²⁶Y.-W. Tang *et al.*, “Laboratory diagnosis of COVID-19: Current issues and challenges,” *J. Clin. Microbiol.* **58**(6), e00512–e00520.
- ²⁷R. Dittadi, H. Afshar, and P. Carraro, “The early antibody response to SARS-CoV-2 infection,” *Clin. Chem. Lab. Med.* **58**(10), e201–e203 (2020).
- ²⁸J.-L. Wu *et al.*, “Four point-of-care lateral flow immunoassays for diagnosis of COVID-19 and for assessing dynamics of antibody responses to SARS-CoV-2,” *J. Infect.* **81**(3), 435–442 (2020).
- ²⁹E. Eteshola and D. Leckband, “Development and characterization of an ELISA assay in PDMS microfluidic channels,” *Sens. Actuators B* **72**(2), 129–133 (2001).
- ³⁰T. Guo *et al.*, “Smartphone dongle for simultaneous measurement of hemoglobin concentration and detection of HIV antibodies,” *Lab Chip* **15**(17), 3514–3520 (2015).
- ³¹P. Novo *et al.*, “Microspot-based ELISA in microfluidics: Chemiluminescence and colorimetry detection using integrated thin-film hydrogenated amorphous silicon photodiodes,” *Lab Chip* **11**(23), 4063–4071 (2011).
- ³²K. A. Heyries *et al.*, “Microfluidic biochip for chemiluminescent detection of allergen-specific antibodies,” *Biosens. Bioelectron.* **23**(12), 1812–1818 (2008).
- ³³J. Yakovleva, R. Davidsson, A. Lobanova, M. Bengtsson, S. Eremin, T. Laurell, and J. Emnéus, “Microfluidic enzyme immunoassay using silicon microchip with immobilized antibodies and chemiluminescence detection,” *Anal. Chem.* **74**(13), 2994–3004 (2002).
- ³⁴A. Zubair *et al.*, “Microfluidic LIPS for serum antibody detection: Demonstration of a rapid test for HSV-2 infection,” *Biomed. Microdevices* **13**(6), 1053–1062 (2011).
- ³⁵Y. Gao *et al.*, “Development of a novel electrokinetically driven microfluidic immunoassay for the detection of *Helicobacter pylori*,” *Anal. Chim. Acta* **543**(1–2), 109–116 (2005).
- ³⁶Y. Bai, C. G. Koh, M. Boreman, Y.-J. Juang, I.-C. Tang, L. James Lee, and S.-T. Yang, “Surface modification for enhancing antibody binding on polymer-based microfluidic device for enzyme-linked immunosorbent assay,” *Langmuir* **22**(22), 9458–9467 (2006).
- ³⁷A. Singhal, C. A. Haynes, and C. L. Hansen, “Microfluidic measurement of antibody-antigen binding kinetics from low-abundance samples and single cells,” *Anal. Chem.* **82**(20), 8671–8679 (2010).
- ³⁸K. Duan, G. Ghosh, and J. F. Lo, “Optimizing multiplexed detections of diabetes antibodies via quantitative microfluidic droplet array,” *Small* **13**(46), 1702323 (2017).
- ³⁹X. Wen, H. He, and L. J. Lee, “Specific antibody immobilization with biotin-poly(L-lysine)-g-poly(ethylene glycol) and protein A on microfluidic chips,” *J. Immunol. Methods* **350**(1–2), 97–105 (2009).
- ⁴⁰M. Cretich *et al.*, “Detection of allergen specific immunoglobulins by microarrays coupled to microfluidics,” *Proteomics* **9**(8), 2098–2107 (2009).
- ⁴¹A. E. Herr, D. J. Throckmorton, A. A. Davenport, and A. K. Singh, “On-chip native gel electrophoresis-based immunoassays for tetanus antibody and toxin,” *Anal. Chem.* **77**(2), 585–590 (2005).
- ⁴²E. A. Redman *et al.*, “Integrated microfluidic capillary electrophoresis-electrospray ionization devices with online MS detection for the separation and characterization of intact monoclonal antibody variants,” *Anal. Chem.* **87**(4), 2264–2272 (2015).
- ⁴³H. Nygren, “Kinetics of antibody binding to surface-immobilized antigen. Analysis of data and an empirical model,” *Biophys. Chem.* **52**(1), 45–50 (1994).
- ⁴⁴C.-Y. Xue, S. A. Khan, and K.-L. Yang, “Exploring optical properties of liquid crystals for developing label-free and high-throughput microfluidic immunoassays,” *Adv. Mater.* **21**(2), 198–202 (2009).

- ⁴⁵Q. Zhu and K. L. Yang, "Microfluidic immunoassay with plug-in liquid crystal for optical detection of antibody," *Anal. Chim. Acta* **853**, 696–701 (2015).
- ⁴⁶J.-W. Choi, K. W. Oh, A. Han, N. Okulan, C. Ajith Wijayawardhana, C. Lannes, S. Bhansali, K. T. Schlueter, W. R. Heineman, H. Brian Halsall, J. H. Nevin, A. J. Helmicki, H. Thurman Henderson, and C. H. Ahn, "Development and characterization of microfluidic devices and systems for magnetic bead-based biochemical detection," *Biomed. Microdevices* **3**, 191–200 (2001).
- ⁴⁷W. Liang *et al.*, "A novel microfluidic immunoassay system based on electrochemical immunosensors: An application for the detection of NT-proBNP in whole blood," *Biosens. Bioelectron.* **31**(1), 480–485 (2011).
- ⁴⁸C. Zhao and X. Liu, "A portable paper-based microfluidic platform for multiplexed electrochemical detection of human immunodeficiency virus and hepatitis C virus antibodies in serum," *Biomicrofluidics* **10**(2), 024119 (2016).
- ⁴⁹S. V. Pereira, G. A. Messina, and J. Raba, "Integrated microfluidic magnetic immunosensor for quantification of human serum IgG antibodies to *Helicobacter pylori*," *J. Chromatogr. B Analyt. Technol. Biomed. Life Sci.* **878**(2), 253–257 (2010).
- ⁵⁰Y. F. Lee *et al.*, "An integrated microfluidic system for rapid diagnosis of dengue virus infection," *Biosens. Bioelectron.* **25**(4), 745–752 (2009).
- ⁵¹S. V. Pereira *et al.*, "A microfluidic device based on a screen-printed carbon electrode with electrodeposited gold nanoparticles for the detection of IgG anti-*Trypanosoma cruzi* antibodies," *Analyst* **136**(22), 4745–4751 (2011).
- ⁵²S. V. Pereira *et al.*, "Microfluidic immunosensor with gold nanoparticle platform for the determination of immunoglobulin G anti-*Echinococcus granulosus* antibodies," *Anal. Biochem.* **409**(1), 98–104 (2011).
- ⁵³C. F. Jofre *et al.*, "Electrochemical microfluidic immunosensor based on TES-AuNPs@Fe₃O₄ and CMK-8 for IgG anti-*Toxocara canis* determination," *Anal. Chim. Acta* **1096**, 120–129 (2019).
- ⁵⁴M. Seia *et al.*, "Laser-induced fluorescence integrated in a microfluidic immunosensor for quantification of human serum IgG antibodies to *Helicobacter pylori*," *Sens. Actuators B* **168**, 297–302 (2012).
- ⁵⁵L. Lafleur *et al.*, "Progress toward multiplexed sample-to-result detection in low resource settings using microfluidic immunoassay cards," *Lab Chip* **12**(6), 1119–1127 (2012).
- ⁵⁶B. S. Lee *et al.*, "A fully automated immunoassay from whole blood on a disc," *Lab Chip* **9**(11), 1548–1555 (2009).
- ⁵⁷Z. Swank *et al.*, "A high-throughput microfluidic nano-immunoassay for detecting anti-SARS-CoV-2 antibodies in serum or ultra-low volume dried blood samples," *Clin. Trials Week* (2020), p. 145.
- ⁵⁸R. Funari, K. Y. Chu, and A. Q. Shen, "Detection of antibodies against SARS-CoV-2 spike protein by gold nanospikes in an opto-microfluidic chip," *Biosens. Bioelectron.* **169**, 112578 (2020).
- ⁵⁹C. Fan *et al.*, "A portable and power-free microfluidic device for rapid and sensitive lead (Pb²⁺) detection," *Sensors* **12**(7), 9467–9475 (2012).
- ⁶⁰X. L. Liu, Y. Z. Wang, and Y. J. Song, "Visually multiplexed quantitation of heavy metal ions in water using volumetric bar-chart chip," *Biosens. Bioelectron.* **117**, 644–650 (2018).
- ⁶¹Y. S. Huang *et al.*, "Target-responsive DNAzyme cross-linked hydrogel for visual quantitative detection of lead," *Anal. Chem.* **86**(22), 11434–11439 (2014).
- ⁶²Y. J. Song *et al.*, "Multiplexed volumetric bar-chart chip for point-of-care diagnostics," *Nat. Commun.* **3**, 1283 (2012).
- ⁶³G. Wang *et al.*, "Microfluidic particle dam for visual and quantitative detection of lead ions," *ACS Sens.* **5**(1), 19–23 (2020).
- ⁶⁴L. T. Chu *et al.*, "Visual detection of lead ions based on nanoparticle-amplified magnetophoresis and Mie scattering," *Sens. Actuators B* **306**, 127564 (2020).
- ⁶⁵M. Wu *et al.*, "Cascade-amplified microfluidic particle accumulation enabling quantification of lead ions through visual inspection," *Sens. Actuators B* **324**(1), 128727 (2020).